Available online at www.sciencedirect.com
SCIENCE DIRECT®
Journal of Power Sources 145 (2005) 101–107
JOURNAL OF POWER SOURCES
www.elsevier.com/locate/jpowsour

Characterisation of zirconium and titanium phosphates and direct methanol fuel cell (DMFC) performance of functionally graded Nafion(R) composite membranes prepared out of them

F. Bauer*, M. Willert-Porada

Chair of Materials Processing, University of Bayreuth, Universitätsstr. 30, D-95447 Bayreuth, Germany

Accepted 28 January 2005
Available online 31 May 2005

Abstract

Pure layered phosphates of varying crystalline phases and crystallinity and composites of gradient layers of zirconium phosphate in Nafion 117-membranes have been prepared. The proton conductivity and, in case of the composites, also the dynamic mechanical properties of these materials were measured under different conditions of temperature and humidity. Membrane-electrode assemblies with low platinum catalyst loading of 0.4 mg cm^{-2} Pt at the cathode and 1.9 mg cm^{-2} Pt–Ru at the anode were examined in a direct methanol fuel cell (DMFC) at medium temperatures (130 °C). The conductivity of the layered zirconium phosphates is superior to the titanium phosphates and increases with decreasing crystallite size. The electrical performance of the composites in a DMFC-environment is slightly decreased as compared to the unmodified membrane but taking the reduced methanol crossover into account, higher efficiencies can be reached with the zirconium phosphate modified membrane. Furthermore, the mechanical properties are significantly improved by the presence of the inorganic compound.

Keywords: Direct methanol fuel cell; Layer phosphate; Proton conductivity; Dynamic mechanical analysis; Composite membrane

1. Introduction

In the last decade significant improvements of the polymer electrolyte membrane fuel cell (PEMFC) were achieved [1–4]. Besides the fuel cell system each of the stacks components, i.e. membrane, catalysts, gas diffusion layer and bipolar plate have been progressed. Of particular importance for enhanced overall efficiency are new composite membranes with significantly decreased thickness, reduced water swelling and at the same time high mechanical strength [5] and electrodes with reduced fraction of platinum group catalysts. Sufficient power density was achieved already with loadings as low as 0.05 mg cm^{-2} catalyst due to an improved number of three-phase contacts [6].

In spite of these advancements, PEMFC power sources have not found broad entrance to the market yet. The available membrane is concerned the available materials show sufficient ionic conductivity only at high water activity, therefore limiting the operating temperature, long time stability, solvent permeability and mechanical stability to values too low for most mobile as well as stationary applications. Besides the three major goals followed in the membrane and electrode development (I) reduction of the noble metal catalyst loading, (II) increase of the operating temperature and (III) increase of long-term stability the membrane, also lower fuel permeability, better chemical and mechanical stability and higher conductivity at low water activities are of crucial importance.

At present no monolithic membrane material is available to fulfill all these requirements. Composite materials, i.e. materials consisting of several components, each contributing its specific advantages to the overall performance, could be a promising alternative. An example for such a composite is an ion conducting organic polymer membrane, which contains inorganic fillers. In such a composite, the organic material

* Corresponding author. Tel.: +49 921 557 203; fax: +49 921 557 205.
E-mail address: felix.bauer@uni-bayreuth.de (F. Bauer).

0378-7753/$ – see front matter © 2005 Elsevier B.V. All rights reserved.
doi:10.1016/j.jpowsour.2005.01.063

should provide the proton conductivity whereas the inorganic component should enhance the membranes mechanical stability, reduce the fuel crossover and improve the performance at low water activities. During the last years there were numerous reports about such composite materials [7–15], a recent review is given by Qingfeng et al. [1].

Within the work presented here, ionic conductivity and phase stability of pure zirconium phosphate and some related layer phosphates were investigated. The most promising inorganic compound, zirconium phosphate, was used as inorganic additive to prepare membranes with the perfluorinated polymer Nafion 117-membrane as matrix. Such composite membranes were characterized in terms of mechanical stability, conductivity and fuel crossover and compared with the unmodified Nafion 117 material.

2. Experimental

2.1. Preparation of layer phosphates

2.1.1. Preparation of zirconium phosphates

(I) A 1 M aqueous solution of $ZrOCl_2 \cdot 8\ H_2O$ (Chempur) was slowly added to a 10 M excess of 1 M H_3PO_4. The precipitate was washed several times with de-ionized water, dried 2 h at 95 °C and stored at 100% RH and room temperature (a-ZP-08). (II) A 1 M solution of zirconium *n*-propylate (Chempur) in *n*-propanol was slowly added to a 10 M excess of 1 M H_3PO_4. The precipitate was washed several times with de-ionized water, dried 2 h at 95 °C and stored at 100% RH and room temperature (a-ZP-21).

2.1.2. Preparation of titanium phosphates

(I) A 0.6 M aqueous solution of $TiOSO_4 \cdot H_2SO_4 \cdot H_2O$ (Aldrich) was slowly added to a 10 M excess of 1 M H_3PO_4. The precipitate was washed several times with de-ionized water, dried 2 h at 95 °C and stored at 100% RH and room temperature (a-TP-37). (II) Fifty millilitres of a 0.35 M solution of titanium *n*-butylate (Chempur) in xylene were slowly added to a slurry of 50 mmol water free H_3PO_4 in xylene. The slurry was refluxed for 2 h and then homogenized in an ultrasonic bath. The resulting white powder was filtered, washed several times with ethanol and stored at 100% RH and room temperature (a-TP-13). (III) A 200 mg of a-TP-13 were refluxed in de-ionized water. The precipitate was washed several times with de-ionized water, dried 2 h at 95 °C and stored at 100% RH and room temperature (d-TP-20). (IV) A 200 mg of a-TP-13 were refluxed in 1.5 M sulfuric acid. The precipitate was washed several times with de-ionized water, dried 2 h at 95 °C and stored at 100% RH and room temperature (d-TP-09).

2.2. Preparation of composites

Commercially available membranes, Nafion® 117 (DuPont, 180 μm thick membranes, Nafion 1100, Aldrich Chemicals) were employed. In order to remove impurities and arrive at comparable starting conditions the membranes were boiled in 10% nitric acid for 2 h, then rinsed several times with de-ionized water to remove excess acid. The membranes were stored under de-ionized water and dried for 1 h at 80 °C in static air prior to use. For the introduction of 8–25 wt.% zirconyl phosphate a method described by Tiwari et al. [16] was used: pre-treated Nafion® membranes were soaked in 0.06 M zirconyl oxychlorid-methanol solution ($ZrOCl_2 \cdot 8\ H_2O$, Riedel de Haen) for a certain amount of time and washed off in methanol. Then, the samples were immersed in 8 wt.% phosphoric acid solution for 1 h and dried for 1 h at 80 °C. This procedure was repeated several times to enlarge the inorganic content of the membrane. To complete hydrolysis and ensure full protonation the membrane was boiled in 1.5 M sulfuric acid for 1 h and rinsed several times in de-ionised water. According to this procedure two membranes containing 13 and 21 wt.% zirconium phosphate (N117-ZP-13, N117-ZP-21) were prepared, where the soaking step in the zirconyl oxychlorid-methanol solution took 15 min without washing off in methanol and one membrane containing 26 wt.% zirconium phosphate (N117-ZP-26) where the soaking step took 4 h and the washing off in methanol took 20 s.

2.3. X-ray diffractometry

X-ray diffraction patterns were recorded in the reflected radiation mode, using a Philips X-PERT system with a Cu Kα radiation source operating at 40 kV and 40 mA. The sample powders were kept at room temperature and 50% RH for at least 24 h prior to the measurement and spread on a microscope slide without further preparation. The scans were carried out under ambient conditions. The crystallite size was calculated from the full width at half maximum of the respective strongest peak around 25° 2θ according to a method described by Scherrer [17].

2.4. He-pycnometry

The skeletal density of the layer phosphates was determined by means of He-pycnometry. Prior to the measurements the samples were dried over P_2O_5 at room temperature for several days. The 10 ml sample tube of a Micromeritics AccuPyc 1330 He-pycnometer was calibrated empty and with two tungsten carbide volumetric standard bodies. Then, about 1 g of sample was transferred to the sample tube. Helium was used as testing gas.

2.5. Impedance spectroscopy

Impedance measurements were carried out by means of a Hewlett Packard HP 4284A LCR meter. Two different methods were used to prepare the membranes and the inorganic pellets, respectively.

2.5.1. Preparation of membrane-electrode assemblies

Appropriate pieces of the membrane were dipped in a slurry consisting of 200 mg carbon supported platinum (E-TEK, DeNora, 20 wt.% Pt), 1 ml Nafion ionomer solution (DuPont, 5 wt.% Nafion 1100) and a mixture of 2 ml water and 2 ml *i*-propanol. The solvents were allowed to evaporate under ambient conditions and the membrane was hot pressed between two Teflon sheets for one minute at 135 °C. Then, pieces of 5 mm diameter were punched out of the catalyst-coated membrane.

2.5.2. Preparation of phosphate-electrode assemblies

The sample pellets consisted of three layers, i.e. one inorganic layer sandwiched between two composite electrode layers. A 100 μl of water and 100 mg of the layer phosphate were ground in a small agate mortar and allowed to dry for 15 min. A 20 mg of the ground powder was mixed with 10 mg carbon supported platinum (E-TEK, DeNora, 20 wt.% Pt) and a drop of Nafion ionomer solution (DuPont, 5 wt.% Nafion 1100) was added. The electrode powder mixture was ground again and allowed to dry for 15 min. Three to four milligrams of the electrode composite were slightly compacted at the bottom of a plunger in a cylindrical die. Then, 40 mg of layer phosphate were piled up above the composite layer and slightly compacted. Finally, 3–4 mg of the electrode composite were piled up above the layer phosphate. According to that procedure samples of 5 mm diameter and about 1 mm thickness were manufactured at a pressure of 10 kN and a pressure duration of 30 s. After removal from the mould the side surface of the pellets was cleaned from carbon residue by lapping.

A conductivity measurement cell similar to that described by Alberti et al. [18] was used. All samples were kept at room temperature and 100% RH for at least 1 week and contacted with electrically conductive gas diffusion layers (SGL Carbon GDL10BB type) of the same diameter on both sides prior to the measurement. The gas-diffusion-layer/sample-assembly was placed between two polished gold plates of the measurement cell and fixed by application of a constant pressure of 0.7 MPa using a steel spring. Immediately before each conductivity measurement a short- and a load-compensation (0.250 Ω resistor) was carried out. The equilibration time between two data points was set to 21/2 h. Conductivity was measured between 80 and 130 °C and 20–100% RH, starting at the highest humidity value. The membrane resistance was derived from the data by performing a nonlinear least square fit to the circuit description code (RQ)QC using the software Equivalent Circuit 4.55 from B. A. Boukamp.

2.6. Dynamic mechanical analysis

The mechanical properties were studied on a dynamic mechanical analyzer DMA 2980, TA Instruments. The top part of the commercial instrument and the top sample holder were replaced by an in-house built humidity cell which has been described in detail elsewhere [19]. The mechanical properties were measured at a frequency of 1 Hz with a static force of 0.25 N and 15.0 μm amplitude between room temperature and 100 °C. All humidity scans were performed in humidified nitrogen atmosphere at variable temperature and humidity. Samples with typical dimensions 26 mm × 6 mm and 200 μm thickness (water saturated state) were fixed at the bottom using a film clamp holder provided by the instrument manufacturer and at the top using the in-house built equipment.

2.7. Cell performance testing

2.7.1. Membrane-electrode assembly (MEA)

Slurries containing 300 mg carbon supported Pt–Ru (E-TEK, DeNora, 60 wt.% Pt–Ru), 2.4 g Nafion ionomer solution (DuPont, 5 wt.% Nafion 1100), 6 ml water and 5 ml isopropanol and 150 mg carbon supported Pt (E-TEK, DeNora, 30 wt.% Pt), 0.6 g Nafion ionomer solution (DuPont, 5 wt.% Nafion 1100), 4 ml water, 3 ml *i*-propanol and 45 mg PTFE-solution (ElectroChem, 65 wt.%) were prepared for the anode and the cathode, respectively. These slurries were sprayed on the microporous layer of gas diffusion layers (SGL Carbon GDL10BB type) using an airbrush spray nozzle and a computer controlled *x*–*y* plotter. The catalyst loading was determined gravimetrically. The anode loading was 1.85 mg cm^{-2} Pt–Ru, the cathode loading was 0.37 mg cm^{-2} Pt. Pieces of 28 mm × 28 mm were cut out of the catalyst coated diffusion layers and Nafion ionomer solution was sprayed onto the electrodes until the dry weight of the ionomer coating amounted to 1.2 mg cm^{-2}. Then, the electrodes were hot pressed onto the membrane at 135 °C, 10 kN for 4 min.

2.7.2. Fuel cell operating conditions

An in-house built single cell testing station was used to examine the performance of the membranes under DMFC conditions and to determine the membrane resistance and the methanol crossover under working conditions. The catalyst coated membrane area was 7.84 cm^2. Meander shaped graphite flow fields were used at both anode and cathode side. Gaskets made of PTFE foils were used to seal the cell. The cell was operated at 130 °C. A 1.5 M aqueous methanol solution was supplied to the anode from a BECKMAN 110 B solvent delivery module at a feed rate of 1.5 ml min^{-1}, a temperature of 130 °C and a constant overpressure of 3.6 bar. Air or oxygen, humidified at 90 °C, was supplied to the cathode at a constant overpressure of 3.6 bar and a feed rate of 400 ml min^{-1} air or 100 ml min^{-1} oxygen, respectively. The current–voltage plots were recorded using an electronic load (ZAHNER elektrik, EL101) connected to an electrochemical workstation (ZAHNER elektrik, IM6e).

2.7.3. Membrane resistance

The impedance of the fuel cell under a constant current density of 0.25 A cm^{-2} was measured in the frequency range between 0.1 Hz and 20 kHz. The cell resistance was set equal to the high frequency intersect of the Nyquist plot with the

Table 1
Phase composition and crystallite size of layer phosphates before and after the conductivity scans

Sample	Phase composition		Crystallite size (nm)	
	Before	After	Before	After
a-ZP-08	α-$Zr(HPO_4)_2 \cdot H_2O$	α-$Zr(HPO_4)_2 \cdot H_2O$	8	8
a-ZP-21	α-$Zr(HPO_4)_2 \cdot H_2O$	α-$Zr(HPO_4)_2 \cdot H_2O$	35	21
a-TP-13	δ-$Ti_4H_{11}(PO_4)_9 \cdot xH_2O$	α-$Ti(HPO_4)_2 \cdot H_2O$	23	13
a-TP-37	α-$Ti(HPO_4)_2 \cdot H_2O$ + UP	α-$Ti(HPO_4)_2 \cdot H_2O$ + UP	11	37
d-TP-09	δ-$Ti_4H_{11}(PO_4)_9 \cdot xH_2O$	Amorphous	9	–
d-TP-20	δ-$Ti_4H_{11}(PO_4)_9 \cdot xH_2O$	δ-$Ti_4H_{11}(PO_4)_9 \cdot xH_2O$ + amorphous	20	–

UP: unknown phase.

real part axis. Ohmic drop by the metallic and graphite components of the cell and their contacts was measured without membrane. It was found to be less than 5% of the lowest resistance measured using the single cell with a MEA and therefore was neglected.

2.7.4. Methanol crossover

The CO_2 concentration of the cathode exhaust gas was measured as a function of current density using a CO_2 infrared detector (Vaisala, GMT221). An ice bath cooled water trap between fuel cell and transmitter was used to dry the exhaust gas stream. The methanol crossover was calculated assuming complete oxidation of the permeated methanol to CO_2 at the cathode. CO_2 crossover was neglected since it was found that at the diffusion limiting current where all methanol arriving at the anode is oxidised the CO_2 signal of the transmitter dropped to zero.

3. Results and discussion

3.1. Characterization of layer phosphates

The phase composition and crystallite size of the layer phosphates was determined by X-ray diffractometry. In order to detect structural changes under conditions similar to that in a working fuel cell the samples were examined before and after the conductivity measurements. The hydrothermal treatment during the measurements in the conductivity cell corresponded to 25 h at 100 °C, 2.2 bar and humidity between 20 and 100% RH. The results are listed in Table 1. Whereas the titanium layer phosphate a-TP-13 has undergone a complete phase transition, as shown in Fig. 1, the treatment of a-TP-13 in boiling water and sulfuric acid induced stabilization of the δ-phase and so d-TP-20 remained unaltered as δ-phase. In contrast to these phases, d-TP-09 has lost crystallinity and the sample became amorphous.

The crystallite size as determined by the Scherrer method ranged between 8 and 37 nm. Concerning the changes in the volume fraction of the crystalline phase, no obvious trend is visible upon hydrothermal treatment. In most cases the cristallinity decreased or remained constant, with exception of the α-$Ti(HPO_4)_2 \cdot H_2O$-phase (a-TP-37), which showed a significantly increased crystallinity.

The observed behaviour can only reflect the thermal stability of the layer phosphates in humid atmosphere. In the environment of the membrane matrix in an operating fuel cell the phosphates are additionally exposed to sterical hindrance, acidic moieties of the ionomer and electric field.

The majority of layer phosphates: a-TP-13, a-TP-37, a-ZP-08, d-TP-09, d-TP-20, show additional reflections between 5° and 10° 2θ in the diffraction pattern, which could not be attributed to known phases (Fig. 1). Most probably these reflections belong to expanded layers of the respective layer phosphates, since it is known that the interlayer peak is shifted to lower 2θ (°) values with increasing water or solvent content, because the interlayer distance increases [20,21]. In case of the titanium phosphates prepared by the precipitation reaction between titanium butylate and phosphoric acid (a-TP-13, d-TP-09, d-TP-20) the additional peak appeared between 5.25° and 5.75° 2θ before and after the hydrothermal treatment. Although all the precipitated samples were washed several times and boiled in water and sulfuric acid, formation of butanol-layer phosphate intercalates might be an explanation for this peak. The interlayer peak for the corresponding α-$Zr(HPO_4)_2$ butanol is found at 4.7° 2θ [21]. In case of the other compounds, the additional peak appeared between 8.6° and 10° 2θ and was assigned to partly hydrated species of the respective phase.

The impedance measurement of the inorganic samples must be regarded with caution since the impedance behaviour depends on many factors. Not only chemical composition, crystallite structure and size, temperature and humidity

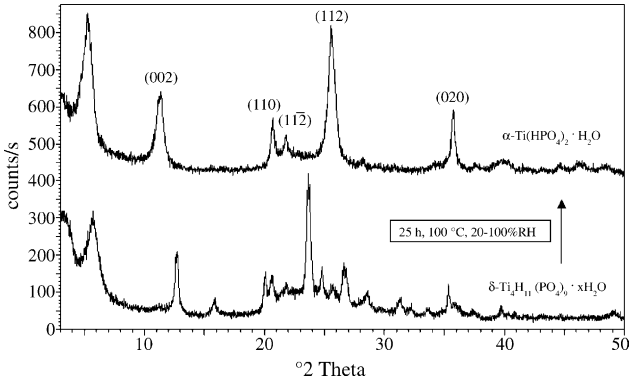

Fig. 1. Diffraction pattern of titanium layer phosphate a-TP-13 before and after the conductivity measurement at 100 °C.

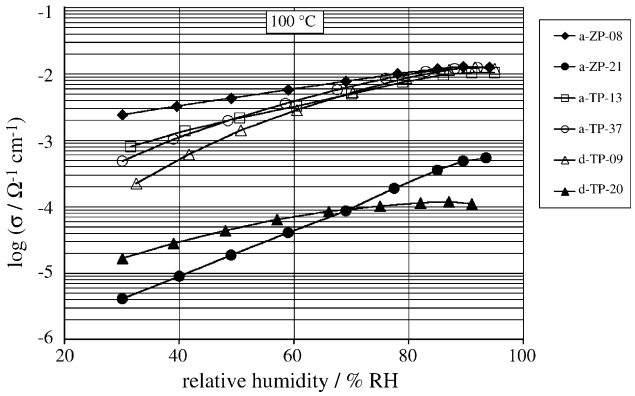

Fig. 2. Proton conductivity of titanium and zirconium layer phosphates of varying morphology and crystallinity as a function of humidity.

influence the impedance behaviour but also morphological parameters like porosity, surface area and agglomerate structure. Therefore, the porosity of the pellets has been calculated by taking the ratio of the geometric density and the skeletal density. The geometric and skeletal densities of all samples ranged between 1.7–2.0 and 2.0–2.4 g cm^{-3}, respectively. The porosity ranged between 13 and 19% for all samples except a-ZP-21, where 29% were calculated. The proton conductivity of the layer phosphates was measured at 100 °C between 20 and 100% RH. The data are presented in Fig. 2. The graphs can be divided into two groups, one having similar conductivity at high humidity but different slopes and one having a significantly lower conductivity. The α-$Zr(HPO_4)_2{\cdot}H_2O$, a-ZP-08 shows the highest conductivity at all humidity values, with the maximum value of 0.013 Ω^{-1} cm^{-1} at 94% RH.

A phase with the same composition but a higher crystallite size (a-ZP-21) shows a conductivity decreased by more than a factor of 10. According to Alberti et al. the proton transport in α-$Zr(HPO_4)_2{\cdot}H_2O$ takes place mostly at the surface of the crystallites, and bulk transport plays only a minor role [22]. Therefore for small crystallite sizes corresponding to a high surface area an increased proton conductivity should be observed. On the other hand the significantly higher porosity of the pellet could cause a reduction of proton conductive paths and explain the decrease.

The conductivity of titanium phosphates depends much more upon humidity, lower conductivity as compared to the zirconium phosphate is found at the highest humidity and a significant decrease of conductivity occurs at low humidity. In case of the a-TP-20 sample, the strong reduction of conductivity could be attributed to a depletion of acidic surface groups after the treatment in boiling water.

3.2. Charactersation of composite membranes

The zirconium layer phosphate had the highest proton conductivity among the different inorganic phases and therefore was used to prepare composite membranes with Nafion 117 as matrix. Two different groups of membranes were prepared:

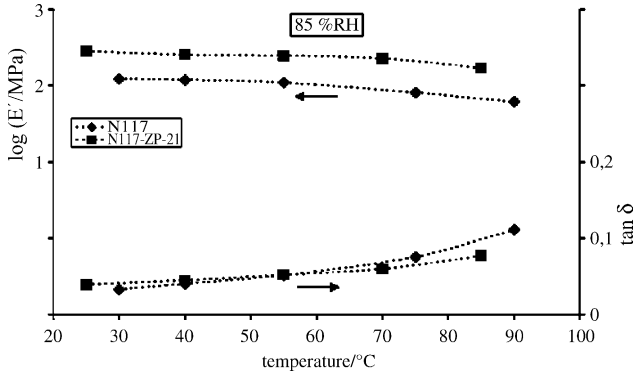

Fig. 3. E' and tan δ of Nafion 117-H (N117) and a Nafion zirconium phosphate composite (N117-ZP-21) vs. temperature at 85% RH.

membranes with the zirconium phosphate mainly residing at the membrane surface (N117-ZP-13, N117-ZP-21) and a membrane with the inorganic phase only present in the inner part of the composite membrane (N117-ZP-26). Zirconium phosphate deposited under these conditions forms the α-phase, as has been verified by the composites diffraction pattern [8].

The dynamic mechanical properties of unmodified Nafion 117 (N117) and a Nafion 117-membrane containing 21 wt.% zirconium phosphate (N117-ZP-21) were compared under constant humidity as well as isothermal conditions, as shown in Figs. 3 and 4. At 85% RH E' of the modified membrane is two to three times higher over the examined temperature range as compared to the unmodified membrane. The onset of the glass transition of the ionic regions of Nafion 117 above 100 °C is indicated by the increasing slope of tan δ at higher temperatures. The isothermal plot exhibits increased E' and decreased tan δ in case of the composite membrane. The stiffening effect of the layer phosphate increases with decreasing humidity.

The mechanical behaviour at variable methanol vapor pressures was measured at 65 °C, as shown in Fig. 5. A similar behaviour was observed as compared to the water humidity isotherm. Methanol is a more effective softener than water with respect to Nafion. Lower values of E' and higher

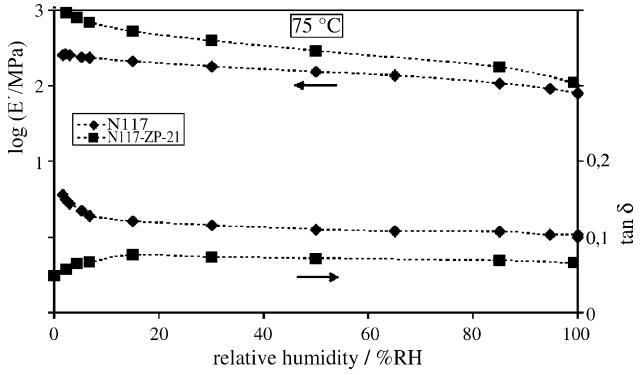

Fig. 4. E' and tan δ of Nafion 117-H (N117) and a Nafion zirconium phosphate composite (N117-ZP-21) vs. humidity at 75 °C.

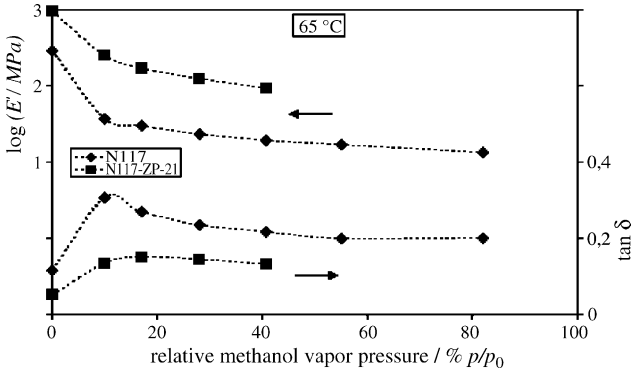

Fig. 5. E' and tan δ of Nafion 117-H (N117) and a Nafion zirconium phosphate composite (N117-ZP-21) vs. methanol vapor pressure at 65 °C.

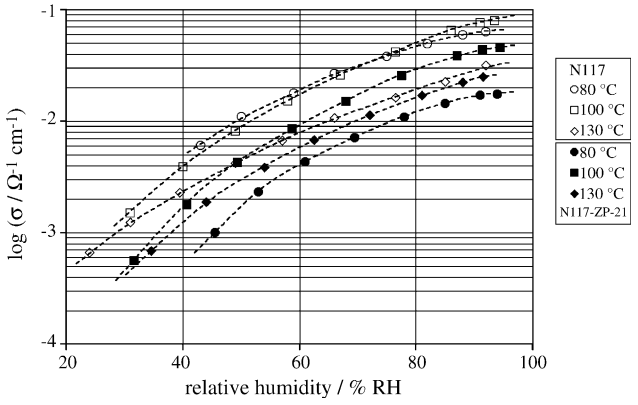

Fig. 6. Proton conductivity of Nafion 117-H (N117) and a Nafion zirconium phosphate composite (N117-ZP-21) vs. humidity at 80, 100 and 130 °C.

tan δ as compared to the hydrated membranes were measured. The stiffening effect of zirconium phosphate in methanol-atmosphere is stronger than in water-humidified atmosphere.

The proton conductivity of unmodified (N117) and composite Nafion 117 (N117-ZP-21) was measured isothermally at three different temperatures, 80, 100 and 130 °C, respectively, as shown in Fig. 6. The presence of the inorganic compound decreased the proton conductivity in all cases. At high humidity the conductivity first increased from 80 to 100 °C and decreased at 130 °C. This behaviour has already been described by Alberti et al. for Nafion 117 [18]. The conductivity decrease is more pronounced in case of the unmodified Nafion and therefore at temperatures above 130 °C the measured values for the inorganically modified and the unmodified membrane approach the same value. At humidity above 50% RH the proton conductivity of the composite is

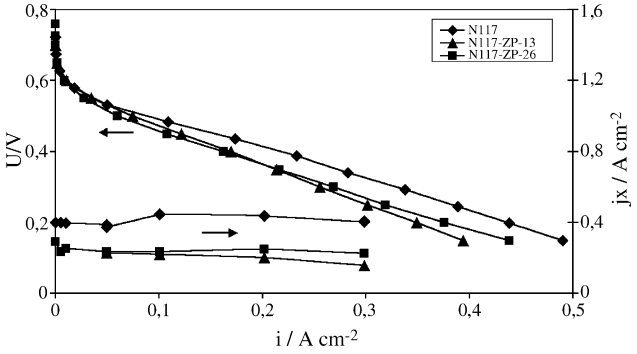

Fig. 7. Performance plot and methanol crossover current of Nafion 117-H (N117) and Nafion zirconium phosphate composites (N117-ZP-13, N117-ZP-26). DMFC operating conditions, anode: Pt–Ru 1.85 mg cm^{-2} 4.6 bar 1.5 mol dm^{-3} methanol, cathode: Pt 0.37 mg cm^2 4.6 bar 400 ml min^{-1} air, cell: 130 °C.

intermediate between the data for the pure zirconium layer phosphate and the data measured for Nafion 117, as shown in Fig. 2.

Cell performance tests were carried out for unmodified Nafion 117 (N117) and two composites (N117-ZP-13, N117-ZP-26). The methanol crossover current was measured under the same conditions as the current–voltage curve and is plotted against the second y-axis, as shown in Fig. 7. The membrane electrical resistance was measured in situ by means of impedance spectroscopy and is compared to the proton conductivity data shown in Fig. 6. The results are listed in Table 2. The power output of Nafion 117 was higher than that of the composites under the same conditions.

3.3. DMFC-performance of graded membranes

The performance plot of the DMFC-testing is presented in Fig. 7. Only slight differences between the two different phosphate concentration gradients of N117-ZP-13 and N117-ZP-26 were observed. At highest current densities the membrane with the inner phosphate layer had a slightly improved performance as compared to the membrane with the layer phosphate close to the surface. The crossover current was reduced by a factor of two as compared to the unmodified Nafion. The rest potentials of the different membranes are listed in Table 2. Both composite membranes exhibited a higher rest potential than unmodified Nafion, which also indicates lower methanol permeability. The conductivity-measured ex situ was significantly lower than the in situ measured values, although indicating the same trend with respect to humidity and

Table 2
Comparison between ex situ and in situ measured proton conductivity at 130 °C and DMFC rest potential of Nafion 117 and composite Nafion membranes

Sample	Zirconium phosphate fraction/wt.%	$\sigma_{ex\ situ}$ (Ω^{-1} cm^{-1}, 92 % RH)	$\sigma_{in\ situ}$ (Ω^{-1} cm^{-1}, liquid H_2O)	U_0/V
N117	0	0.032	0.150	0.725
N117-ZP-13	13	–	0.088	0.768
N117-ZP-21	21	0.025	–	–
N117-ZP-26	26	–	0.084	0.760

temperature. The differences can be explained by the different water activity in the conductivity measurement chamber (92% RH at 2.2 bar) and the fuel cell (liquid water at 4.6 bar). The proton conductivity of Nafion rises sharply when the membrane is transferred from water vapor into liquid water [23].

4. Conclusions

Different layer phosphates of zirconium and titanium were characterized by their X-ray diffraction pattern and their conductivity. The α-$Zr(HPO_4)_2 \cdot H_2O$ with the lowest crystallinity exhibited the highest conductivity. The δ-phase of the titanium phosphate is unstable under hydrothermal conditions and converts to the α-phase.

The mechanical properties of the zirconium phosphate composite proof that the inorganic filler acts as a stiffener. In the examined range of temperature and humidity the stiffening effect depends weakly on the temperature and strongly on humidity. This applies to humid atmosphere as well as to methanol vapor atmosphere. The proton conductivity is reduced by the inorganic filler. At temperatures above 130 °C the difference in conductivity levels out for modified as compared to unmodified membranes. The electrical performance of the composites in a DMFC-environment is slightly decreased as compared to the unmodified membrane but taking methanol crossover into account, higher efficiencies can be reached with the zirconium phosphate modified Nafion 117-membrane as compared to the organic membrane. Furthermore, mechanical properties of the membrane are improved by the inorganic fillers.

Acknowledgements

Financial support by the Deutsche Forschungsgemeinschaft (DFG) under the contract number Wi 856/13-2 and Wi 856/13-3 is gratefully acknowledged.

References

[1] L. Qingfeng, H. Ronghuan, J.O. Jensen, N.J. Bjerrum, Chem. Mat. 15 (2003) 4896–4915.
[2] S. Wasmus, A. Küver, J. Electroanal. Chem. 461 (1999) 14–31.
[3] C. Heitner-Virguin, J. Membr. Sci. 120 (1996) 1–33.
[4] S. Surampudi, S.R. Narayanan, E. Vamos, H. Frank, G. Halpert, A. LaConti, J. Kosek, G.K.S. Prakash, G.A. Olah, J. Power Sources 47 (1994) 377–385.
[5] J.A. Kolde, B. Bahar, M.S. Wilson, T.A. Zawodzinski, S. Gottesfeld, Advanced composite polymer electrolyte fuel cell membranes, in: S. Gottesfeld, G. Halpert, A. Landgrebe (Eds.), Proton Conducting Membrane Fuel Cells, Proceedings of the first International Symposium on Proton Conducting Fuel Cells I, The Electrochemical Society, 1995, pp. 193–201.
[6] Q. Zhigang, A. Kaufman, J. Power Sources 114 (2003) 21–31.
[7] C. Yang, S. Srinivasan, A.B. Bocarsly, S. Tulyani, J.B. Benziger, J. Membr. Sci. 237 (2004) 145–161.
[8] F. Bauer, M. Willert-Porada, J. Membr. Sci. 233 (2004) 141–149.
[9] A.S. Arico, V. Baglio, A. Di Blasi, E. Modica, P.L. Antonucci, V. Antonucci, J. Power Sources 128 (2004) 113–118.
[10] S.P. Nunes, B. Ruffmann, E. Rikowski, S. Vetter, K. Richau, J. Membr. Sci. 203 (2002) 215–225.
[11] O.J. Murphy, A.J. Cisar, US 6,387,230 B1 (2002) 1–16.
[12] P. Costamagna, C. Yang, A.B. Bocarsly, S. Srinivasan, Electrochim. Acta 47 (2002) 1023–1033.
[13] K.T. Adjemian, S.J. Lee, S. Srinivasan, J. Benziger, A.B. Bocarsly, J. Electrochem. Soc. 149 (2002) A256–A261.
[14] S.K. Young, K.A. Mauritz, J. Polym, Sci. Part B: Polym. Phys. 39 (2001) 1282–1295.
[15] C. Yang, S. Srinivasan, A.S. Aricò, P. Cretì, V. Baglio, V. Antonucci, Electrochem. Solid-State. Lett. 4 (2001) A31–A34.
[16] S.K. Tiwari, S.K. Nema, Y.K. Agarwal, Thermochim. Acta 317 (1998) 175–182.
[17] H. Krischner, B. Koppelhuber-Bitschnau, Röntgenstrukturanalyse und Rietveldmethode, Vieweg, Braunschweig/Wiesbaden (1994).
[18] G. Alberti, M. Casciola, L. Massinelli, B. Bauer, J. Membr. Sci. 185 (2001) 73–81.
[19] F. Bauer, S. Denneler, M. Willert-Porada, J. Polym. Sci., Part B: Polym. Phys. 43 (2005) 786–795.
[20] E. Skou, I.G.K. Andersen, E.K. Andersen, Solid State Ionics 35 (1989) 59–65.
[21] D.E.C. Corbridge, Phosphorus: An Outline of its Chemistry, Biochemistry and Technology, Elsevier, Amsterdam, 1995.
[22] G. Alberti, M. Casciola, U. Costantino, G. Levi, G. Ricciardi, J. Inorg. Nucl. Chem. 40 (1978) 533–537.
[23] T.A. Zawodzinski Jr., T.E. Springer, F. Uribe, S. Gottesfeld, Solid State Ionics 60 (1993) 199–211.